SLAC-PUB-17224
February 2018

HE-LHC Optics Development

Yunhai Cai and Yuri Nosochkov*
SLAC National Accelerator Laboratory, Menlo Park, CA, USA
Mail to: yuri@slac.stanford.edu

Massimo Giovannozzi, Thys Risselada, Ezio Todesco, Demin Zhou*
and Frank Zimmermann
CERN, Route de Meyrin, 1211 Geneva 23, Switzerland
* KEK, Tsukuba, Japan
Mail to: dmzhou@post.kek.jp, frank.zimmermann@cern.ch

1 Introduction

The High Energy LHC (HE-LHC) proton-proton collider is a proposed replacement of the LHC [1] in the existing 27-km tunnel, with the goal of increasing a centre-of-mass (CM) beam energy from 14 to 27 TeV. Some of the challenges of this machine are:

- A factor of almost two higher dipole field
- Higher field in quadrupoles and sextupoles
- Attaining sufficient dynamic aperture (DA) in presence of potentially larger field errors
- Fitting the ring close to the present LHC layout

The nominal LHC arc magnets have the aperture of 56 mm, and provide the field up to 8.33 T in dipoles, 223 T/m in quadrupoles, and 4430 T/m^2 in sextupoles [1]. The high field required at the HE-LHC beam energy can be realized by taking advantage of the magnet technology being developed for the 100-km FCC-hh design [2]. The latter aims at reaching 16 T field in dipoles, 400 T/m gradient in quadrupoles, and 7800 T/m^2 in sextupoles, where the magnet aperture is 50 mm [3,4]. Scaling of the present LHC to 27 TeV CM energy yields the magnet field exceeding the FCC specifications. Therefore, a new lattice design is required.

Design of the FCC 16-T dipole is based on Nb_3Sn superconductor; this however may potentially degrade the field quality (FQ), compared to the LHC dipole based on Nb-Ti superconductor. Further FQ degradation may be caused by a large swing between the HE-LHC injection and collision energies, and due to the slightly smaller magnet aperture. The resulting larger non-linear field errors may limit the ring dynamic aperture, especially at injection energy, where the field errors are typically larger than at collision energy as well as the beam size. The quadrupole and sextupole strengths increase with the energy, but also depend on beam optics. It is desirable to minimize the strengths of these magnets for the HE-LHC, so the cost-effective Nb-Ti technology could be used, wherever possible.

2 Lattice Design

As a first step of designing the HE-LHC lattice, we consider a simplified model of injection lattice with realistic arcs, but simple Interaction Regions (IR) without dipoles. Later, we apply the realistic IR layout with dipoles, specific to each location.

* Work supported by the US Department of Energy contract DE-AC02-76SF00515.

Published in ICFA Beam Dynamics Newsletter, No. 72, p. 141-151, December 2017

The two rings of the present LHC consist of eight octants, where each octant contains an arc made of twenty three 90° FODO cells, a dispersion suppressor at each arc end, and an IR. The rings cross each other four times as shown in Fig. 1, hence there are four long and four short arcs in each ring. Beam focusing is anti-symmetric with respect to each Interaction Point (IP), so the two beams see the same optics pattern. Layout of the simplified HE-LHC model represents approximately the average layout of the two LHC rings, as shown in blue in Fig. 1. The model arcs are of the same (average) length, the IRs are straight without dipoles, and the ring has four-fold optics symmetry.

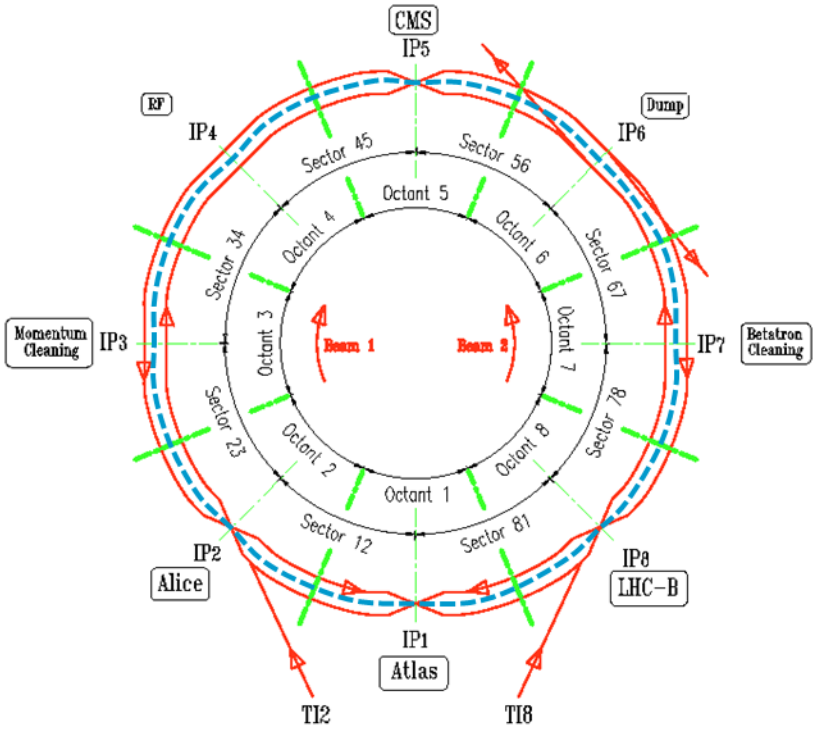

Figure 1: Layout of two LHC rings with long and short arcs (red); and schematic of simplified HE-LHC model with average length arcs and straight IRs (blue dash).

2.1 *Design strategy*

The goal of the HE-LHC lattice design is to minimize the magnet strengths and reduce the impact of non-linear field errors on dynamic aperture. Two methods are considered for the reduction of the magnet strengths in the arcs:

- A lower phase advance μ_c per arc FODO cell, and
- A longer arc cell L_c (the number of arc cells is reduced as $N_c \sim 1/L_c$)

Both of these methods, however, increase dispersion in the arcs; moreover a longer cell yields larger beta functions ($\sim L_c$). The resulting larger beam size may be more challenging for the collimation system, and a larger momentum compaction factor may require higher RF voltage.

The proposed strategy to reduce the effects of non-linear field errors is to choose the number of arc cells and the cell phase advance such that $N_c\mu_c = 2\pi\times$integer [5-7]. This provides cancellation of second-order effects from periodic sextupoles and suppression of many non-linear resonances driven by systematic non-linear field errors in the periodic arcs. As a result, looser tolerances on the field quality may be acceptable.

2.2 *Lattice models*

Several injection lattice models have been designed having the following common features:

- Circumference C = 26658.8832 m, identical to the LHC
- Ring closely fits the LHC ring geometry
- FODO cell arc optics
- Same quadrupole and sextupole lengths and magnet-to-magnet distances as in the LHC
- One type dipole in arcs and dispersion suppressors
- Dipole length is within the acceptable limit of 14.3 m
- Simplified IR layout without dipoles
- Anti-symmetric optics relative to each IP, as in the LHC
- Fractional tune of 0.28/0.31 as in the LHC injection lattice
- Arc phase advance of $N_c\mu_c = 2\pi\times$integer in most models

Parameters of the designed lattices are shown in Table 1, where the LHC injection lattice V6.503 is included for comparison. The strengths of arc magnets are scaled to 13.5 TeV to determine the required maximum field. The dipole and quadrupole strengths of the nominal LHC exceed the FCC limits of 16 T and 400 T/m, respectively; therefore, this lattice is not considered for the HE-LHC. The dipole length and the fill factor in the modeled arc cells are maximized for the lowest dipole field, assuming the same quadrupole and sextupole lengths and magnet-to-magnet distances as in the LHC. With the latter conditions, longer cells yield a lower dipole field. For a strict limit of 16 T field in dipoles, including a small operational margin, only the models with 18 cells per arc in Table 1 qualify for further consideration.

All the models satisfy the FCC field limit in arc quadrupoles and sextupoles. Their strengths are lower in longer cells with a lower phase advance. The sextupole strength, however, may increase in collision optics due to large chromaticity created in the low-beta IR1 and IR5.

Matching the circumference and fitting the ring layout is done by optimizing the lengths of the arc cell and the dispersion suppressor. The resulting trajectory offsets relative to the LHC are typically within 10 cm. The three ring models with 18 cells per arc, shown in Table 1, have identical geometry.

Peak beta functions are proportional to the cell length, and only minor affected by the cell phase advance within the 60° to 90° range. Peak dispersion quadratically increases with the cell length, and strongly increases as the phase advance is reduced. Cell optics functions in the 18×60° and 18×90° arcs are shown in Fig. 2 for comparison.

Dispersion suppressor connects the arc and the IR, and consists of two FODO cells with 8 dipoles. The design is based on the LHC layout, where adjustments are made to the cell and dipole lengths. As in the LHC, the optics match between the arc and the IR is done using the dispersion suppressor quadrupoles and the two quadrupoles in the adjacent arc cell. The IR dispersion is fully cancelled in the designed models.

For the injection lattice, we use a simplified IR layout without dipoles, and injection-type IR optics with small beta functions. This design should be adequate for the study of dynamic aperture, since the effects of IR errors are not significant in injection lattice. Example of the IR and dispersion suppressor optics for 18×90° model is shown in Fig. 3, where the IP beta function is 15 m. The complete ring optics is shown in Fig. 4. Geometrically, the model ring is eight-fold symmetric having identical

octant layouts. The optics, however, is four-fold symmetric since the focusing is anti-symmetric with respect to each IP, and hence the quadrupole polarities change sign from octant to octant.

Table 1: Parameters of HE-LHC injection lattice models and the LHC V6.503 injection lattice, where magnet field is at 13.5 TeV beam energy.

	LHC V6.503 23 × 90°	***Model 24 × 60°***	***Model 20 × 90°***	***Model 18 × 60°***	***Model 18 × 80°***	***Model 18 × 90°***
Cells per arc	23	24	20	18	18	18
Cell phase advance, deg	90	60	90	60	80	90
Cell length, m	106.90	102.45	122.94	137.23	137.23	137.23
Dipole length, m	14.3	13.56	12.625	14.18	14.18	14.18
Dipoles per arc cell	6	6	8	8	8	8
Total number of dipoles	1232	1280	1424	1280	1280	1280
Arc dipoles fill factor	0.803	0.794	0.809	0.827	0.827	0.827
Dipole B, T	16.06	16.30	15.92	15.59	15.59	15.59
Arc quad B′, T/m	404.8	289.5	334.8	214.9	276.3	304.0
Sextupole B″, T/m^2	4883	2057	2940	866	1824	2475
Max/Min arc β function, m	184 / 29	177 / 60	208 / 38	237 / 80	228 / 50	233 / 40
Max/Min arc dispersion, m	2.03 / 0.96	3.75 / 2.26	3.0 / 1.5	6.73 / 4.06	4.30 / 2.22	3.64 / 1.75
Tune, x/y	64.28 / 59.31	49.28 / 47.31	55.28 / 54.31	38.28 / 37.31	47.28 / 48.31	54.28 / 53.31
Momentum compaction	$3.22\ 10^{-4}$	$6.41\ 10^{-4}$	$4.70\ 10^{-4}$	$1.12\ 10^{-3}$	$6.83\ 10^{-4}$	$5.58\ 10^{-4}$
Natural chromaticity	-86 / -82	-63 / -63	-73 / -72	-47 / -47	-62 / -63	-73 / -73

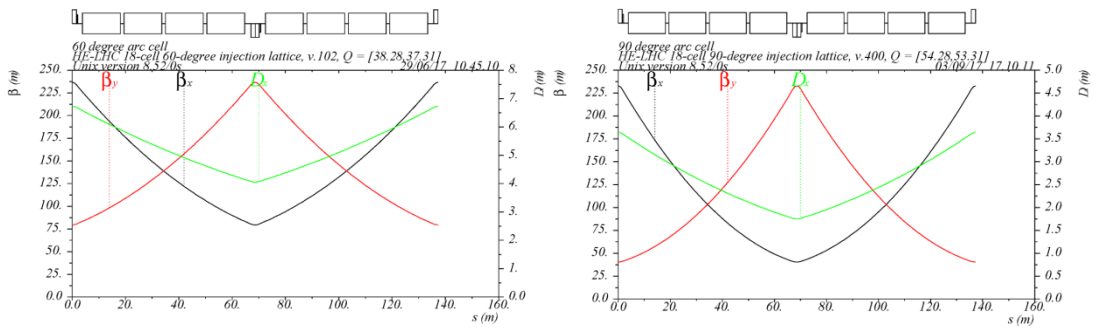

Figure 2: Cell optics functions in the 18×60° (left) and 18×90° arcs (right).

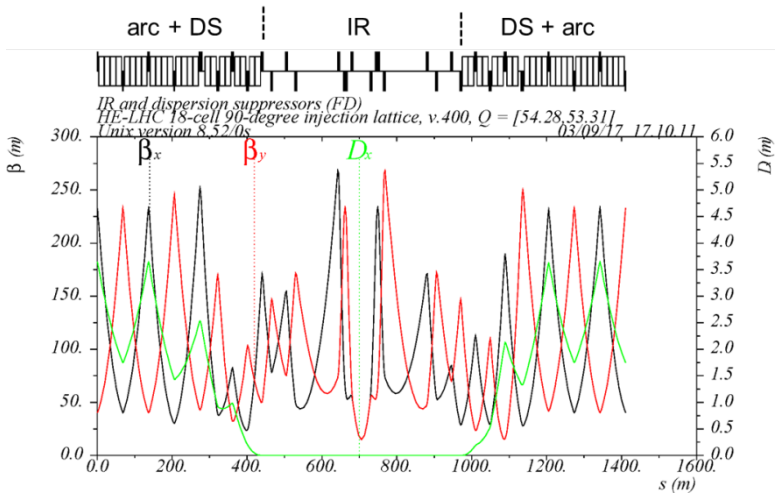

Figure 3: Optics functions in the IR, dispersion suppressors (DS) and the last two arc cells at each arc end in 18×90° model.

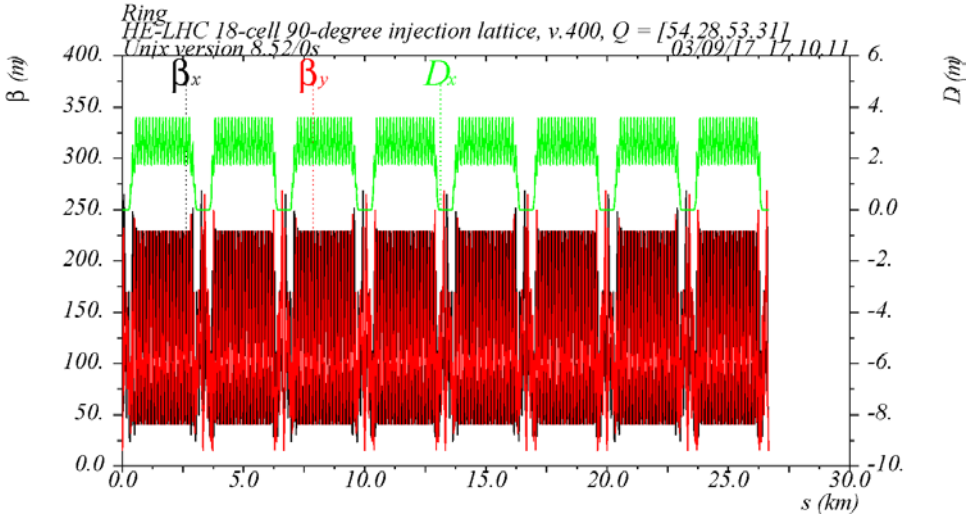

Figure 4: Optics functions in the complete 18×90° injection lattice model with simple IRs.

3 Dynamic Aperture

In view of a possible degradation of the dipole field quality at injection energy, the HE-LHC model lattice includes non-linear field compensation properties. This is implemented by setting the total arc phase advance to $N_c\mu_c = 2\pi\times$integer in both planes (except in the 18×90° model). For a completely periodic arc, this condition results in suppression of many resonances driven by arc sextupoles and systematic non-linear field errors in the arc magnets [5-7]. Figure 5 shows a perfect cancellation of many 3rd order resonance driving terms generated by the periodic arc sextupoles in 18×60° lattice option, where all arc cells are identical.

In the actual lattice design, presented in Table 1, strengths of quadrupoles in the first and the last arc cells are somewhat adjusted to improve the dispersion suppressor match; hence, the optics functions in these cells are not exactly periodic. The result is a deviation from perfect sextupole compensation over the full arc, although the exact

cancellation still holds for a shorter part of the arc corresponding to the number of identical cells where total phase advance is multiple of 2π.

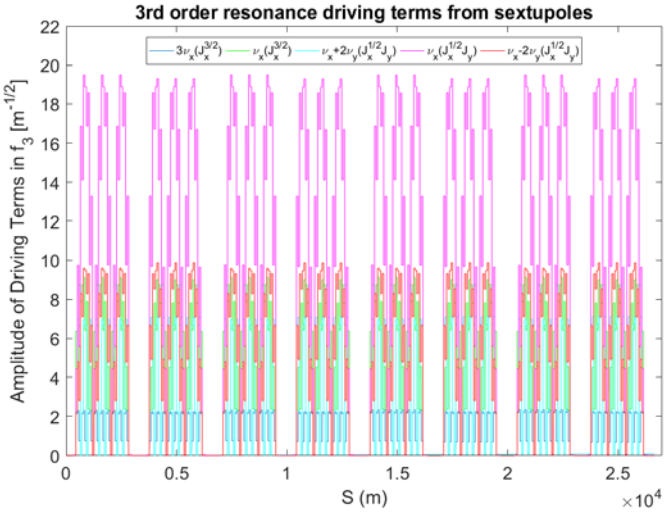

Figure 5: Accumulation and compensation of the 3rd order resonance driving terms from arc sextupoles in 18×60° lattice where all arc cells are identical.

Similarly, compensation of the non-linear effects caused by systematic field errors in dipoles is limited to the periodic cells with total 2π×integer phase advance, while residual effects are expected from dipole errors in the arc matching cells and dispersion suppressors. The lattice model with 18×90° arcs differs from the other models because by design the arc phase advance is not multiple of 2π. In this case, the non-linear field cancellation is limited to the inner 16 cells. This lattice model has more optimal dispersion suppressor optics, since the latter is originally designed for the 90° LHC arcs. The 90° cells are also more readily compatible with the Achromatic Telescopic Squeezing (ATS) scheme for chromatic aberrations compensation [8].

3.1 *Tracking simulations*

The short-term DA of the designed lattice models is evaluated using LEGO [9] and SAD [10] codes. The DA is performed at 450 GeV injection energy and expressed in units of rms beam size for normalized beam emittance of 2.5 μm-rad. Typical tracking simulation is performed for 1024 turns, with initial momentum offset up to 7.5×10^{-4}, and linear chromaticity of +3.

Figure 6 shows DA of the three 18-cell models without errors for the initial momentum offset of $\Delta p/p = 0$ and 7.5×10^{-4}. The DA of all models is significantly larger than the DA of the present LHC injection lattice. This is due to the four-fold symmetry of the simple models resulting in cancellation of many resonances, and built-in non-linear compensation in the arcs which reduce the effects of sextupoles. Without the errors, the DA increases as the cell phase advance is reduced, while the effect of non-zero $\Delta p/p$ is small.

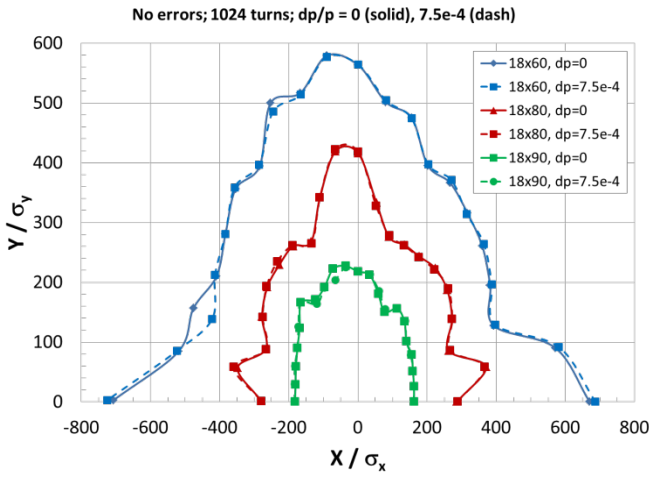

Figure 6: Dynamic aperture of 18×60°, 18×80°, and 18×90° injection lattices without errors for initial momentum offset of $\Delta p/p = 0$ and 7.5×10^{-4}.

3.2 *Non-linear field errors in dipoles*

A possible degradation of dipole field quality at injection energy is a concern for the HE-LHC dynamic aperture. Estimates of the dipole FQ for FCC-hh at injection energy [11] predict that the lowest order allowed field components are in the range of

- $b_{3S} = 7$, $b_{3R} = b_{3U} = 1.6$
- $b_{5S} = 1$, $b_{5R} = b_{5U} = 0.1$
- $b_{7S} = -1.5$, $b_{7R} = b_{7U} = 0.03$,

where *S*, *R* and *U* stand for the systematic, random and uncertainty components, and the reference radius is 17 mm. The full value of b_n is obtained using the formula [12]

$$b_n = b_{nS} + \frac{\xi_U}{1.5} b_{nU} + \xi_R b_R,$$

where ξ_U, ξ_R are random Gaussian values with σ = 1, cut at 1.5 σ and 3 σ, respectively. Here, the ξ_U is the same for all magnets of a given class, but changes from seed to seed and for the different field components; while ξ_R changes from magnet to magnet.

Similar to the LHC correction system, we consider that b_3 and b_5 correctors are included at each dipole to compensate the dipole systematic b_{3S} and b_{5S} errors. However, in this tracking study these correctors are not included. In order to simulate such a correction, we make an assumption that the b_{3S} and b_{5S} errors after correction are effectively reduced to 5% and 30%, respectively, of the values shown above, i.e. the residual $b_{3S} = 0.35$ and $b_{5S} = 0.3$.

Additionally, the LEGO tracking code allows only the systematic and random error components to be included. To take into account the uncertainty component, we make another assumption, where the ξ_U is made random in all magnets, and that the ξ_U and ξ_R are independent. We then combine them into one random component ξ_R corresponding to $b_{3R} = 1.92$, $b_{5R} = 0.12$, and $b_{7R} = 0.036$. These new values along with the systematic components shown above are used in the tracking.

3.3 *Dynamic aperture with dipole field errors*

Impact of the systematic dipole field errors b_{3S}, b_{5S}, and b_{7S} on the DA of 18-cell lattice models is dominated by the b_{5S} and b_{7S} components. The impact of b_{3S} is

relatively small due to the lattice non-linear compensation properties, and the chromaticity correction provided by the sextupoles.

Dynamic aperture with the systematic and random b_3, b_5, b_7 field errors in dipoles for five random seeds is shown in Fig. 7 for the initial $\Delta p/p = 0$ and 7.5×10^{-4}. One can see that the 18×80° and 18×90° models have a larger aperture as compared to the 18×60° model. The aperture is reduced in the case of non-zero momentum offset, but remains sufficient for the 18×80° and 18×90° models. The optimal value of the momentum offset at injection energy needs to be further specified.

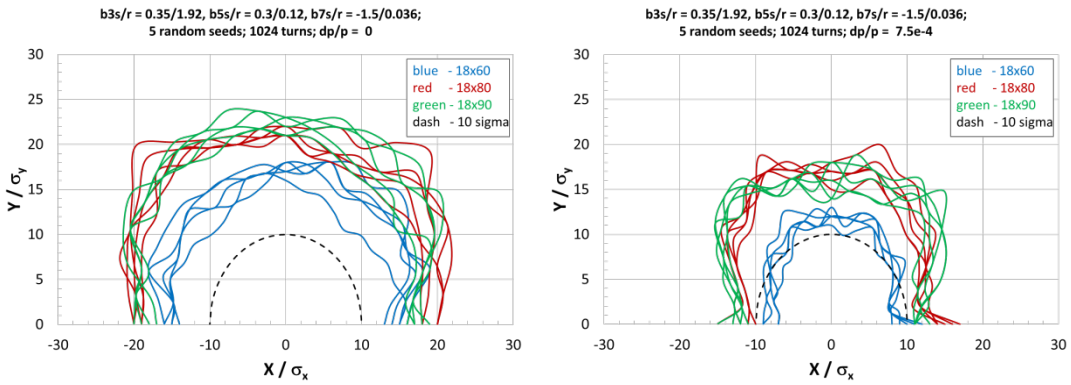

Figure 7: Dynamic aperture of 18×60°, 18×80°, and 18×90° injection lattices with systematic and random b_3, b_5, b_7 field errors in dipoles for the initial $\Delta p/p = 0$ (left) and 7.5×10^{-4} (right) and 5 random seeds.

4 Realistic Injection Lattice Model

Design of the HE-LHC injection lattice with realistic IR layout is in progress. One lattice based on a combination of 18×90° arcs and IR geometry from the SLHCV3.1a lattice layout is designed. The ring is matched to the LHC layout to within about 1 cm accuracy. The complete lattice functions are shown in Fig. 8, where one can see the different optics in different IRs.

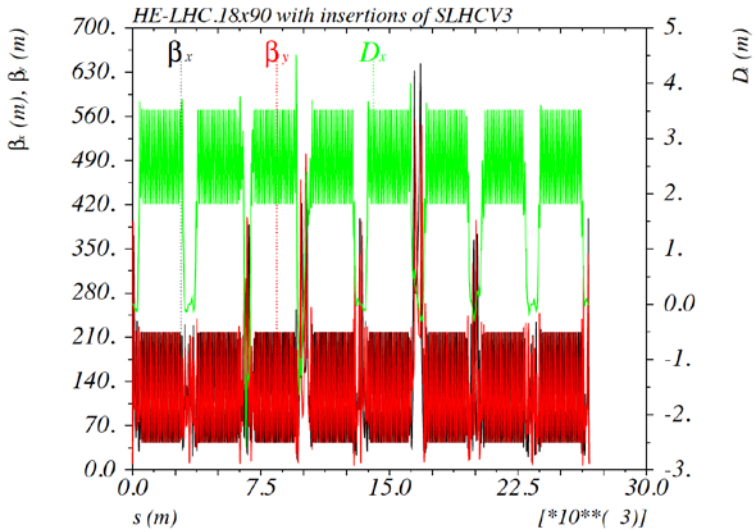

Figure 8: Lattice functions in the HE-LHC injection model with realistic IRs and 18×90° arcs.

The realistic IRs require strong dipoles due to the high 13.5 TeV collision energy and the assumed larger beam separation (204 mm) between the rings in the arcs. These magnets include 12-T D1, D2 and 8-T D3, D4 superconducting dipoles in the IR4, and 1.8 T normal conducting dipoles D3, D4 in the IR3 and IR7. Further optimization of this preliminary IR design is underway.

Dynamic aperture of the realistic lattice without errors is very large, as can be seen in Fig. 9. The tracking is performed using SAD [10] based on standard frequency map analysis algorithm. Since the lattice is based on the 18-cell arcs, the dipole field at top energy is comfortably below the 16 T limit. This realistic design is compatible with the HE-LHC requirements.

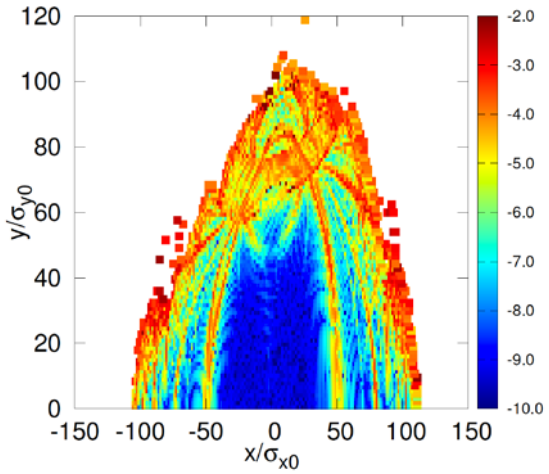

Figure 9: Dynamic aperture of the HE-LHC injection lattice with realistic IRs and 18×90° arcs without errors.

5 Conclusion

Several models of the HE-LHC injection lattice with simple IRs are designed and compared. They feature low magnet strengths and include built-in non-linear field compensation properties in the arcs. The optimal models are based on the 18-cell arcs and cell phase advance of 80° and 90°, yielding sufficient dynamic aperture with the expected dipole field errors. The initial realistic design based on the 18×90° arcs and the IR layout of the SLHCV3.1a lattice is complete. This design satisfies the HE-LHC magnet field requirements, and provides a close match to the LHC ring layout and a large dynamic aperture without errors.

6 References

1. LHC Design Report, Vol. I, 2004.
2. M. Benedikt, F. Zimmermann, “Future Circular Colliders”, in Proceedings of Science, LeptonPhoton2015, 052, and CERN-ACC-2015-0165 (2016).
3. D. Tommasini et al, "The 16 T dipole development program for FCC", IEEE Transactions on Applied Superconductivity, Vol. 27, 4 (2017).
4. D. Schoerling, "Magnet status towards the CDR", FCC Week 2017, Berlin, Germany (2017).
5. K. L. Brown, “A second order magnetic optical achromat”, SLAC-PUB-2257

(1979).
6. A. Verdier, “Resonance free lattices for AG machines”, CERN-SL-99-018-AP, CERN-SL-99-18-AP (1999).
7. Y. Cai, K. Bane, R. Hettel, Y. Nosochkov, M.-H. Wang, M. Borland, “Ultimate storage ring based on fourth-order geometric achromats”, Phys.Rev.ST Accel. Beams 15 054002 (2012).
8. S. Fartoukh, “Achromatic telescopic squeezing scheme and its application to the LHC and its luminosity upgrade”, Phys. Rev. ST Accel. Beams 16, 111002 (2013).
9. Y. Cai, M. Donald, J. Irwin and Y. Yan, “LEGO: a modular accelerator design code”, SLAC-PUB-7642 (1997).
10. http://acc-physics.kek.jp/SAD/index.html.
11. B. Dalena, “Status of dynamic aperture and alignment for FCC-hh”, FCC Week 2017, Berlin, Germany (2017).
12. M. Giovannozzi, S. Fartoukh, R. De Maria, “Specification of a system of correctors for the triplets and separation dipoles of the LHC upgrade”, in Proc. IPAC 2013 Shanghai, China, WEPEA048 (2013).
13. S. Fartoukh, private communication.